

Sub-Architecture Ensemble Pruning in Neural Architecture Search

Yijun Bian, Qingquan Song, Mengnan Du, Jun Yao, Huanhuan Chen, *Senior Member, IEEE*, and Xia Hu

Abstract—Neural architecture search (NAS) is gaining more and more attention in recent years due to its flexibility and remarkable capability to reduce the burden of neural network design. To achieve better performance, however, the searching process usually costs massive computations that might not be affordable for researchers and practitioners. While recent attempts have employed ensemble learning methods to mitigate the enormous computational cost, however, they neglect a key property of ensemble methods, namely diversity, which leads to collecting more similar sub-architectures with potential redundancy in the final design. To tackle this problem, we propose a pruning method for NAS ensembles called “*Sub-Architecture Ensemble Pruning in Neural Architecture Search (SAEP)*.” It targets to leverage diversity and to achieve sub-ensemble architectures at a smaller size with comparable performance to ensemble architectures that are not pruned. Three possible solutions are proposed to decide which sub-architectures to prune during the searching process. Experimental results exhibit the effectiveness of the proposed method by largely reducing the number of sub-architectures without degrading the performance.

Index Terms—ensemble learning, diversity, ensemble pruning, neural architecture search.

I. INTRODUCTION

DESIGNING neural network architectures usually requires manual, laborious architectural engineering, extensive expertise, and high costs. Neural architecture search (NAS), which aims to mitigate these challenges, is attracting increasing attention recently [1]–[3]. However, NAS methods usually require a huge computational effort to achieve an architecture with the expected performance, which is too expensive for many infrastructures and too costly for researchers [4]. Recent work [5]–[7] proposes to employ ensemble methods to mitigate this shortcoming by combining weak sub-architectures trained with lower computational cost into powerful neural architectures. AdaNet, as a prominent example of them, contributes to present a theoretical analysis of the problem of learning both the network architecture and its parameters

simultaneously, and proposes the first generalization bounds for the problem of structural learning of neural networks [5], [8].

However, all of them overlook a crucial principle in ensemble methods (i.e., model diversity) in the search for new sub-architectures, which is usually beneficial for creating better model ensembles [9]–[11]. Besides, lots of ensemble pruning methods exploit the diversity property to obtain sub-ensembles with a smaller size than the original ensembles [12], [13]. It has been proved that a few diverse individual learners could even construct a more powerful ensemble learner than the unpruned ensembles [14], [15]. This motivates us to investigate the NAS ensemble pruning problem, where different sub-ensemble architectures are aligned to a smaller but effective ensemble model. Moreover, it is quite challenging to describe the characteristics of diversity for different sub-architectures and decide which one of them should be pruned or kept in the ensemble architecture. First, there are plenty of definitions or measurements for diversity in the ensemble learning community [15]. Unlike the model accuracy, however, there is no well-accepted formal definition of diversity [16]. Second, diversity among individual learners usually decreases as those individual learners approach higher levels of accuracy [17]. Combining some diverse individual learners with some relatively weak ones is usually better than combining accurate ones only since diversity is more important than pure accuracy. Third, selecting the best combination of sub-architectures from an ensemble architecture is NP-complete hard with exponential computational complexity [18], [19]. Thus, how to manage the trade-off between accuracy and diversity properly, and how to select the best subset of ensemble architectures, is a significant problem in the NAS ensemble pruning problems.

Motivated by the characteristic of diversity in ensemble learning, we strive for diverse sub-ensemble architectures at a smaller size, meanwhile, maintaining comparable accuracy performance to the original ensemble architecture without pruning. The idea is to prune the ensemble architecture on-the-fly based on various criteria and keep more valuable sub-architectures in the searching process. Our NAS ensemble pruning method is named as “*Sub-Architecture Ensemble Pruning in Neural Architecture Search (SAEP)*,” motivated by AdaNet [5] and ensemble pruning methods, with three proposed criteria to decide which sub-architectures to prune. Note that *SAEP* also has some differences from typical ensemble pruning problems, since most pruning methods are usually handled on the original ensemble that has been trained, but pruning in *SAEP* is done in the process of searching rather than after the searching. Moreover, *SAEP* might lead to distinct

Y. Bian and H. Chen are with the School of Computer Science and Technology, University of Science and Technology of China, Hefei 230027, China. E-mails: yjbian@mail.ustc.edu.cn; hchen@ustc.edu.cn

Q. Song, M. Du, and X. Hu are with the Department of Computer Science and Engineering, Texas A&M University, College Station, TX, 77840, United States. E-mails: song_3134@tamu.edu; dumengnan@tamu.edu; hu@cse.tamu.edu

J. Yao is with the Data Science and Analytics Department, WeBank, Shenzhen, 518000, China. E-mail: junyao@webank.com

Manuscript received December 05, 2019; revised May 17, 2020; revised February 12, 2021; accepted May 18, 2021. This research is supported in part by the National Key Research and Development Program of China under Grant No. 2016YFB1000905, the National Natural Science Foundation of China under Grant No. 91746209, and the Fundamental Research Funds for the Central Universities. Corresponding author: Huanhuan Chen.

deeper architectures than the original one if the degree of diversity is insufficient, which could be a bonus due to pruning. Our contribution in this paper is threefold:

- We propose a NAS ensemble pruning method to search sub-ensemble architectures at a smaller size that benefits from an essential characteristic, i.e., diversity in ensemble learning. It could achieve comparable accuracy performance to ensemble architectures that are not pruned.
- Moreover, our proposed method would lead to distinct deeper architectures than the original ensemble architecture that is not pruned if the diversity is insufficient.
- Experimental results exhibit the effectiveness of the proposed method in largely reducing the number of sub-architectures in ensemble architectures and increasing the diversity while maintaining the final performance.

II. PROBLEM STATEMENT

Notations: In this paper, we denote tensors with bold italic lowercase letters (e.g., \mathbf{x}), vectors with bold lowercase letters (e.g., \mathbf{x}), and scalars with italic lowercase letters (e.g., x). We use \mathbf{x}^T to represent the transpose of a vector. Data/hypothesis spaces are denoted by bold script uppercase letters (e.g., \mathcal{X}). We use $\mathbb{R}, \mathbb{P}, \mathbb{E}$, and \mathbb{I} to denote the real space, the probability measure, the expectation of a random variable, and the indicator function, respectively.

We summarize the notations and their definitions in Table I. We follow the notations and the definition of the search space in AdaNet to formulate the problem and introduce the proposed method, as it is one of the most popular ensemble search methods in the NAS literature. It is worth mentioning that the proposed pruning criteria could also be generalized to other ensemble methods, which could be interesting for future research.

Let f be a neural network with l layers searched via AdaNet [5], [8], where each layer would be connected to the previous layers. The output for each $\mathbf{x} \in \mathcal{X}$ would connect to all intermediate units, i.e.,

$$f(\mathbf{x}) = \sum_{1 \leq k \leq l} \mathbf{w}_k \cdot \mathbf{h}_k(\mathbf{x}), \quad (1)$$

where $\sum_{k=1}^l \|\mathbf{w}_k\|_1 = 1$ and $\mathbf{h}_k = [h_{k,1}, \dots, h_{k,n_k}]^T$. $h_{k,j}$ is the function of a unit in the k^{th} layer, i.e.,

$$h_{k,j}(\mathbf{x}) = \sum_{0 \leq s \leq k-1} \mathbf{u}_s \cdot \phi_s(\mathbf{h}_s(\mathbf{x})), \quad k \in [l], \quad (2)$$

where $h_0(\mathbf{x}) = \mathbf{x}$ is the 0^{th} layer denoted by the input. Note that $\phi_s(\mathbf{h}_s)$ denotes that $\phi_s(\mathbf{h}_s) = (\phi_s(h_{s,1}), \dots, \phi_s(h_{s,n_s}))$ where the ϕ_s is assumed to be 1-Lipschitz activation functions, such as the ReLU¹ or sigmoid² function [5]. If $\mathbf{u}_s = 0$ for $s < k-1$ and $\mathbf{w}_k = 0$ for $k < l$, this architecture of f will coincide with the standard multi-layer feed-forward ones [5].

To investigate the search space \mathcal{F} , \mathcal{H}_k is used to denote the family of the function in the k^{th} layer. Let $\tilde{\mathcal{H}}_k \stackrel{\text{def}}{=} \mathcal{H}_k \cup (-\mathcal{H}_k)$ denote the union of \mathcal{H}_k and its reflection, and

¹The Rectified Linear function (ReLU function) [20]–[22] is defined as $g(z) = \max\{0, z\}$.

²The sigmoid function [23] is defined as $\sigma(z) = \frac{1}{1+e^{-z}}$.

TABLE I
THE USED SYMBOLS AND DEFINITIONS IN THIS PAPER.

Notation	Definition
$[n]$	the representation of $\{1, \dots, n\}$ for clarity
$\mathbf{x} \in \mathcal{X}$	the input of neural networks
$f(\cdot) \in \mathcal{F}$	the function of a neural network with l layers
n_s	the number of units in the s^{th} layer
$h_{k,j}(\cdot)$	the function of a unit in the k^{th} layer ($k \in [l]$)
$\mathbf{u}_s \in \mathbb{R}^{n_s}$	the weight of the s^{th} layer for the units of the k^{th} layer
$\mathbf{h}_k(\cdot)$	the function vector of units in the k^{th} layer
$\mathbf{w}_k \in \mathbb{R}^{n_k}$	the weight of the k^{th} layer for $f(\cdot)$
$\ \mathbf{w}_k\ _p$	the l_p -norm of \mathbf{w}_k where $p \geq 1$
$T \geq 1$	the number of iterations in the neural architecture searching process
Γ	a specific complexity constraint based on the Rademacher complexity

let $\mathcal{H} \stackrel{\text{def}}{=} \cup_{k=1}^l \tilde{\mathcal{H}}_k$ denote the union of the families $\tilde{\mathcal{H}}_k$. Then \mathcal{F} coincides with the convex hull of \mathcal{H} , which means that generalization bounds for ensemble methods could be utilized to analyze learning with \mathcal{F} [5]. Therefore, Cortes *et al.* [5], [8] attempted to propose learning guarantees based on a Rademacher complexity analysis [24] to guide their design of algorithms.

While AdaNet attempts to train multiple weak sub-architectures with lower computational costs to comprise powerful neural architectures inspired by ensemble methods [5], the crucial characteristic of diversity brings opportunities to achieve sub-ensemble architectures at a smaller size with diverse sub-architectures, yet still with the comparable performance to an original ensemble architecture generated by AdaNet. Based on the above notions, we formally define the NAS ensemble pruning problem.

Problem Definition (NAS Ensemble Pruning). *Given an ensemble architecture $f(\mathbf{x}) = \sum_{1 \leq k \leq l} \mathbf{w}_k \cdot \mathbf{h}_k(\mathbf{x}) \in \mathcal{F}$ searched by ensemble NAS methods such as AdaNet, and a training set $S = \{(\mathbf{x}_1, y_1), \dots, (\mathbf{x}_m, y_m)\}$ with the size of m , assuming that all training instances are drawn i.i.d. (independently and identically distributed) from a distribution \mathcal{D} over $\mathcal{X} \times \{c_1, \dots, c_{n_c}\}$ with n_c as the number of labels, the goal is to prune the ensemble architecture f and search for a sub-ensemble architecture of a smaller size, while maintaining comparable performance to the original ensemble architecture f .*

III. SUB-ARCHITECTURE ENSEMBLE PRUNING IN NEURAL ARCHITECTURE SEARCH (SAEP)

In this section, we elaborate on the proposed NAS ensemble pruning method to obtain smaller yet effective neural ensemble architectures. Before pruning the less valuable sub-architectures, we need to generate sub-architectures first. We take advantage of AdaNet [5] here due to its popularity and superiority in ensemble NAS research, and utilize its objective function to generate candidate sub-architectures in the searching process. The objective function for generating new candidates in AdaNet is defined as

$$\mathcal{L}_g(\mathbf{w}) = \hat{R}_{S,\rho}(f) + \Gamma, \quad (3)$$

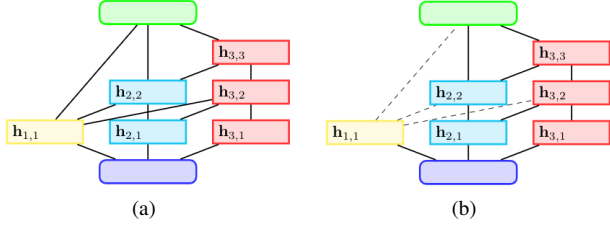


Fig. 1. This figure is used to illustrate the difference between *SAEP* and *AdaNet* during the incremental construction of neural architectures. Layers in blue and green indicate the input and output layers, respectively. Units in yellow, cyan, and red are added at the first, second, and third iteration, respectively. (a) *AdaNet* [5]: A line between two blocks of units indicates that these blocks are fully-connected. (b) *SAEP*: Only some valuable blocks are kept (those that will be pruned are denoted by black dashed lines), which is the key difference from *AdaNet*. The criteria used to decide which sub-architectures will be pruned have three proposed solutions in our *SAEP*, i.e., *PRS*, *PAP*, and *PIE*.

where $\hat{R}_{S,\rho}(f)$ denotes the empirical margin error of function f on the training set S , and Γ denotes a specific complexity constraint.

As the learning guarantee in [5] applies to binary classification, we introduce an auxiliary function $g(\mathbf{x}, y, f)$ in Eq. (4) to extend the objective to multi-class classification problems consistent with our problem statement, i.e.,

$$g(\mathbf{x}, y, f) = 2\mathbb{I}(f(\mathbf{x}) = y) - 1. \quad (4)$$

In this case, the empirical margin error $\hat{R}_{S,\rho}(f)$ would be

$$\hat{R}_{S,\rho}(f) = \frac{1}{m} \sum_{1 \leq i \leq m} \mathbb{I}(g(\mathbf{x}_i, y_i, f) \leq \rho). \quad (5)$$

Guided by Eq. (3), *AdaNet* only generates new candidates by minimizing the empirical error and architecture complexity, while overlooking the diversity and differences among different sub-architectures. To achieve smaller yet effective ensembles via taking the diversity property into account, we need first to measure the diversity of different sub-architectures so that a corresponding objective function could be derived to guide us for the selection of more valuable sub-architectures during the searching process.

Specifically, we propose three different ways to enhance the diversity of different sub-architectures. Except for the first solution, the latter two provide specific objective quantification where diversity is involved as guidance among different sub-architectures for NAS. Besides, the diversity of sub-ensemble architectures generated by them could be quantified to verify whether these ways work or not.

Our final NAS ensemble pruning method, named as “*Sub-Architecture Ensemble Pruning in Neural Architecture Search (SAEP)*,” is shown in Algorithm 1. The key difference between *SAEP* and *AdaNet* is that *SAEP* prunes the less valuable sub-architectures based on certain criteria during the searching process (lines 10–11 in Algorithm 1), instead of keeping all of them, as shown in Figure 1. At the t^{th} iteration ($t \in [T]$) in Algorithm 1, let $f^{(t-1)} = \sum_{1 \leq k \leq l} \mathbf{w}_k \cdot \mathbf{h}_k$ denote the neural network constructed before the start of the t^{th} iteration, with the depth $l^{(t-1)}$ of f . The first target at the t^{th} iteration is to generate new candidates (lines 3–4) and select the better one

Algorithm 1 Sub-Architecture Ensemble Pruning in Neural Architecture Search (*SAEP*)

Input: Dataset $S = (\mathbf{x}_i, y_i)_{i=1}^m$

Parameter: Number of iteration T

Output: Final function $f^{(T)}$

- 1: Initialize $f^{(0)} = \mathbf{0}$, and $l^{(0)} = 1$.
- 2: **for** $t = 1$ **to** T **do**
- 3: $\mathbf{w}', \mathbf{h}' = \operatorname{argmin}_{\mathbf{w}, \mathbf{h}} \mathcal{L}_g(f^{(t-1)} + \mathbf{w} \cdot \mathbf{h})$ s.t. $\mathbf{h} \in \mathcal{H}_{l^{(t-1)}}$.
- 4: $\mathbf{w}'', \mathbf{h}'' = \operatorname{argmin}_{\mathbf{w}, \mathbf{h}} \mathcal{L}_g(f^{(t-1)} + \mathbf{w} \cdot \mathbf{h})$ s.t. $\mathbf{h} \in \mathcal{H}_{l^{(t-1)}+1}$.
- 5: **if** $\mathcal{L}_g(f^{(t-1)} + \mathbf{w}' \cdot \mathbf{h}') \leq \mathcal{L}_g(f^{(t-1)} + \mathbf{w}'' \cdot \mathbf{h}'')$ **then**
- 6: $f^{(t)} = f^{(t-1)} + \mathbf{w}' \cdot \mathbf{h}'$.
- 7: **else**
- 8: $f^{(t)} = f^{(t-1)} + \mathbf{w}'' \cdot \mathbf{h}''$.
- 9: **end if**
- 10: Choose \mathbf{w}_p based on one certain criterion, i.e., picking randomly in *PRS*, $\mathcal{L}_d(\mathbf{w})$ of Eq. (6) in *PAP*, or $\mathcal{L}_e(\mathbf{w}_i)$ of Eq. (16) in *PIE*.
- 11: Set \mathbf{w}_p to be zero.
- 12: **end for**

to be added in the model of $f^{(t-1)}$ (lines 4–9) since we expect the searching process is progressive. The second target at the t^{th} iteration is to prune the less valuable sub-architectures for $f^{(t)}$ and keep beneficial ones to construct the final architecture (lines 10–11).

To evaluate the most valuable sub-architectures, we propose three solutions to tackle this problem. Now we introduce them to decide which sub-architectures are less valuable to be pruned.

A. Pruning by Random Selection (*PRS*)

The first solution, named as “*Pruning by Random Selection (PRS)*,” is to randomly prune some of the sub-architectures in the searching process, with one difference from other solutions. In *PRS*, we firstly decide randomly whether or not to pick one of the sub-architectures to be pruned; if we indeed decide to prune one of them, the objective to decide which sub-architectures to prune is random as well, instead of the specific objective in the next two solutions.

However, there is no specific objective for *PRS* to follow in the pruning process. That might lead to a situation where some valuable sub-architectures are pruned as well. Therefore, we need to find more explicit objectives to guide our pruning.

B. Pruning by Accuracy Performance (*PAP*)

To measure different sub-architectures better, we propose the second pruning solution based on their accuracy performance. This method is named as “*Pruning by Accuracy Performance (PAP)*.” To choose the valuable sub-architectures from those individual sub-architectures in the original model, this second optional objective function for this target is defined as

$$\mathcal{L}_d(\mathbf{w}) = \frac{1}{m} \sum_{1 \leq i \leq m} [g(\mathbf{x}_i, y_i, f) - g(\mathbf{x}_i, y_i, f - \mathbf{w} \cdot \mathbf{h})], \quad (6)$$

where \mathbf{h} is the sub-architecture corresponding to the weight \mathbf{w} . The target is to pick up the \mathbf{w} and \mathbf{h} by minimizing Eq. (6), and prune them if their loss is less than zero. The reason why

we do this is that the generalization error of gathering all sub-architectures is defined as

$$R(f) = \mathbb{E}_{(\mathbf{x}, y) \sim \mathcal{D}} [\mathbb{I}(g(\mathbf{x}, y, f) \leq 0)]; \quad (7)$$

if the j^{th} sub-architecture is excluded from the final architecture, the generalization error of the pruned sub-ensemble architecture will become

$$R(\bar{f}_j) = \mathbb{E}_{(\mathbf{x}, y) \sim \mathcal{D}} [\mathbb{I}(g(\mathbf{x}, y, f - \mathbf{w}_j \cdot \mathbf{h}_j) \leq 0)]. \quad (8)$$

Then, if we expect the pruned architecture works better than the original one, we need to make sure that $R(f) - R(\bar{f}_j) \geq 0$, i.e.,

$$\mathbb{E}_{(\mathbf{x}, y) \sim \mathcal{D}} [g(\mathbf{x}, y, f) - g(\mathbf{x}, y, f - \mathbf{w}_j \cdot \mathbf{h}_j)] \leq 0. \quad (9)$$

Therefore, if the j^{th} sub-architecture meeting Eq. (9) is excluded from the final architecture, the performance will not be weakened and could be even better than the original one. The hidden meaning behind Eq. (9) is that the final architecture makes mistakes; however, the pruned architecture that excludes the j^{th} sub-architecture will work correctly. These sub-architectures that make too serious mistakes to affect the final architecture negatively would be expected to be pruned, leading to our loss function Eq. (6). In this case, we could *improve the performance of the final architecture without breaking the learning guarantee*.

However, this objective in Eq. (6) only considers the accuracy performance of different sub-architectures and misses out on the crucial characteristic of diversity in ensemble methods. Therefore, we need to find an objective to reflect accuracy and diversity both.

C. Pruning by Information Entropy (PIE)

To consider accuracy and diversity simultaneously, we propose another strategy, named “*Pruning by Information Entropy (PIE)*.” The objective is based on information entropy. For any sub-architecture \mathbf{w}_j in the ensemble architecture, $\mathbf{w}_j = \mathbf{w}_j \cdot [\mathbf{h}_j(\mathbf{x}_1), \dots, \mathbf{h}_j(\mathbf{x}_m)]^T$ represents its classification results on the dataset S . $\mathbf{y} = [y_1, \dots, y_m]^T$ is the class label vector. Notice that $H(\cdot)$ and $H(\cdot, \cdot)$ are the entropy function and the joint entropy function, respectively, i.e.,

$$H(\mathbf{w}_i) = - \sum_{w \in \mathbf{w}_i} p(w) \log p(w), \quad (10)$$

$$H(\mathbf{w}_i, \mathbf{y}) = - \sum_{w \in \mathbf{w}_i} \sum_{y \in \mathbf{y}} p(w, y) \log p(w, y). \quad (11)$$

To exhibit the relevance between this sub-architecture and the class label vector, the normalized mutual information [25],

$$\begin{aligned} \text{MI}(\mathbf{w}_i, \mathbf{y}) &= \frac{I(\mathbf{w}_i; \mathbf{y})}{\sqrt{H(\mathbf{w}_i)H(\mathbf{y})}} \\ &= \frac{\sum_{w \in \mathbf{w}_i, y \in \mathbf{y}} p(w, y) \log \frac{p(w, y)}{p(w)p(y)}}{\sqrt{\sum_{w \in \mathbf{w}_i} p(w) \log p(w) \sum_{y \in \mathbf{y}} p(y) \log p(y)}}, \end{aligned} \quad (12)$$

is used to imply its accuracy. Note that

$$\begin{aligned} I(\mathbf{w}_i; \mathbf{y}) &= H(\mathbf{w}_i) - H(\mathbf{w}_i | \mathbf{y}) \\ &= \sum_{w \in \mathbf{w}_i, y \in \mathbf{y}} p(w, y) \log \frac{p(w, y)}{p(w)p(y)}, \end{aligned} \quad (13)$$

is the mutual information [26]. To reveal the redundancy between two sub-architectures (\mathbf{w}_i and \mathbf{w}_j) in the ensemble architecture, the normalized variation of information [25],

$$\begin{aligned} \text{VI}(\mathbf{w}_i, \mathbf{w}_j) &= 1 - \frac{I(\mathbf{w}_i; \mathbf{w}_j)}{H(\mathbf{w}_i, \mathbf{w}_j)} \\ &= 1 - \frac{\sum_{w \in \mathbf{w}_i, y \in \mathbf{y}} p(w, y) \log \frac{p(w, y)}{p(w)p(y)}}{- \sum_{w \in \mathbf{w}_i, y \in \mathbf{y}} p(w, y) \log p(w, y)}, \end{aligned} \quad (14)$$

is used to indicate the diversity between them. The objective function for handling the trade-off between diversity and accuracy of two sub-architectures is defined as

$$\mathcal{L}_p(\mathbf{w}_i, \mathbf{w}_j) = (1 - \alpha) \text{VI}(\mathbf{w}_i, \mathbf{w}_j) + \alpha \frac{\text{MI}(\mathbf{w}_i, \mathbf{y}) + \text{MI}(\mathbf{w}_j, \mathbf{y})}{2}, \quad (15)$$

if $\mathbf{w}_i \cdot \mathbf{h}_i \neq \mathbf{w}_j \cdot \mathbf{h}_j$, otherwise $\mathcal{L}_p(\mathbf{w}_i, \mathbf{w}_j) = 0$. Note that α is a regularization factor introduced to balance between these two criteria, indicating their importance as well. Our target is to pick up the \mathbf{w} and \mathbf{h} , and prune them by minimizing $\mathcal{L}_e(\mathbf{w})$ in Eq. (16), i.e.,

$$\mathcal{L}_e(\mathbf{w}_i) = \sum_{\mathbf{w}_j \cdot \mathbf{h}_j \in f \setminus \{\mathbf{w}_i \cdot \mathbf{h}_i\}} \mathcal{L}_p(\mathbf{w}_i, \mathbf{w}_j). \quad (16)$$

This loss function considers both diversity and accuracy concurrently according to the essential characteristics in ensemble learning.

IV. EXPERIMENTAL STUDY

In this section, we describe the experiments to verify the effectiveness of the proposed *SAEP* method. There are four major questions that we aim to answer. (1) Could *SAEP* achieve sub-ensemble architectures at a smaller size yet still with comparable accuracy performance to the original ensemble architecture? (2) Could *SAEP* generate sub-ensemble architectures with more diversity than the original ensemble architecture? (3) What are the impacts of the parameter α on the sub-ensemble architectures generated by *PIE*? (4) Could *PIE* generate different sub-architectures from that in the original ensemble architecture?

A. Three Image Classification Datasets

The three image classification datasets that we employ in the experiments are all publicly available. The ImageNet [28] dataset is not included since the cost for it is not affordable for one GPU (NVIDIA GTX 1080) that we use.

CIFAR-10 [29]: 60,000 32x32 color images in 10 classes are used as instances, with 6,000 images per class, representing airplanes, automobiles, birds, cats, deer, dogs, frogs, horses, ships, and trucks, respectively. There are 50,000 training images and 10,000 test images.

MNIST [30]: 70,000 28x28 grayscale images of handwritten digits in 10 different classes are used as instances. There are 60,000 instances as a training set and 10,000 instances as a test set. The digits have been size-normalized and centered in a fixed-size image.

Fashion-MNIST [31]: 70,000 28x28 grayscale images are used as instances, including 60,000 instances for training and 10,000 instances for testing. They are categorized into ten classes, representing T-shirts/tops, trousers, pullovers, dresses,

TABLE II

EMPIRICAL RESULTS OF ENSEMBLE-ARCHITECTURES' PERFORMANCE FOR BINARY CLASSIFICATION ON CIFAR-10, FASHION-MNIST, AND MNIST DATASETS. EACH METHOD INCLUDES THREE COLUMNS, I.E., THE *test accuracy (%)*, THE *size of generated (sub-)ensemble architectures*, AND THE *time cost (min)* OF THE SEARCHING PROCESS. THE BEST OF THEM ARE INDICATED WITH BOLD FONTS FOR EACH LABEL PAIR (ROW). NOTE THAT SUB-ARCHITECTURES USED IN THESE EXPERIMENTS ARE MLPs.

Label Pair				Test Accuracy (%)						
	AdaNet	PRS	PAP	PIE	AdaNet.W	PRS.W	PAP.W	PIE.W		
digits 6-9	99.85±0.07	99.83±0.05	99.85±0.07	99.85±0.09	99.84±0.05	99.88±0.04†	99.84±0.14†	99.83±0.07		
digits 5-8	99.14±0.13	99.18±0.21	99.19±0.18	99.21±0.10†	99.16±0.18	99.26±0.15	99.19±0.18	99.20±0.15		
top-pullover	97.03±0.47	97.06±0.15†	97.03±0.39†	97.04±0.34†	97.04±0.30†	97.16±0.18†	97.08±0.21†	96.94±0.17		
top-coat	98.62±0.14	98.57±0.29†	98.61±0.07	98.64±0.32	98.61±0.22†	98.61±0.22†	98.66±0.23	98.67±0.14		
top-shirt	85.87±0.77	86.36±0.82	86.33±0.77†	86.18±0.80	86.14±0.54†	86.48±0.62†	86.27±0.69†	86.36±0.54†		
trouser-dress	98.35±0.16	98.42±0.16	98.39±0.17	98.38±0.28	98.30±0.14	98.39±0.14†	98.41±0.27	98.32±0.24†		
sandal-ankle boot	98.74±0.19	98.78±0.27	98.79±0.24	98.71±0.11	98.78±0.14†	98.71±0.10	98.69±0.19	98.69±0.31†		
deer-truck	87.91±0.38	88.01±0.42	87.87±0.85†	87.99±0.67	87.95±0.35†	88.05±0.47	87.93±0.40	87.91±0.49		
deer-horse	75.54±1.45	76.22±1.17†	76.22±1.07†	76.62±0.94†	76.10±1.28†	76.31±1.15†	76.22±0.41†	76.25±0.46†		
automobile-truck	72.93±0.24	72.82±0.57†	72.91±0.29†	72.84±0.85†	72.58±0.94†	72.78±0.50†	72.90±0.81†	72.95±1.10		
cat-dog	61.15±0.69	61.11±0.23	61.02±1.24†	60.67±1.05†	61.63±0.81	61.60±0.68†	61.22±0.47†	61.53±1.34		
dog-horse	78.21±0.30	77.95±1.02†	78.29±0.61	78.44±0.23†	78.20±0.81†	78.41±0.71	78.23±0.98	78.38±0.95		
t-test (W/T/L)	—	3/7/2	3/6/3	2/6/4	3/4/5	2/4/6	2/6/4	2/8/2		
Average Rank	5.71	4.75	4.71	3.92	5.58	2.67	4.25	4.42		

[†] The reported results are the average values of each method and the corresponding standard deviation under 5-fold cross-validation on each dataset.
[‡] By two-tailed paired t-test at 5% significance level, † and ‡ denote that the performance of AdaNet is inferior to and superior to that of the comparative SAEP method with their variants, respectively.
[‡] The last two rows show the results of t-test and average rank, respectively. The “W/T/L” in t-test indicates that AdaNet is superior to, not significantly different from, or inferior to the corresponding comparative SAEP methods including their variants. The average rank is calculated according to the Friedman test [27].

(a) Comparison on the *test accuracy (%)* performance.

Label Pair				Number of Sub-Architectures						
	AdaNet	PRS	PAP	PIE	AdaNet.W	PRS.W	PAP.W	PIE.W		
digits 6-9	4.20±1.47	5.80±0.40	6.00±0.89	5.80±0.98	6.20±0.98	5.20±1.17	5.60±0.49	5.00±1.79†		
digits 5-8	6.80±0.40	6.00±0.63†	6.60±0.49	5.80±0.75	6.00±0.63†	6.20±1.17	5.60±0.49†	6.00±1.10		
top-pullover	5.00±0.63	5.40±0.49	5.80±0.98†	5.20±0.98†	5.00±0.89	3.80±1.17	4.20±0.75	3.20±0.40†		
top-coat	5.40±0.80	4.80±0.40†	4.60±0.80†	5.40±0.80	5.20±0.75†	5.40±0.49†	4.40±0.80	3.00±0.00†		
top-shirt	5.60±0.49	5.40±0.80	5.60±0.80	5.20±1.47	5.60±1.02	5.80±0.75†	4.20±0.98	4.60±1.62		
trouser-dress	4.20±1.47	5.20±0.75	5.20±1.17	4.40±1.36	5.00±1.10	4.00±1.79	4.00±0.63†	4.60±1.62†		
sandal-ankle boot	5.20±0.75	5.80±1.17†	5.40±1.02†	5.40±1.36†	6.20±0.75†	5.40±0.49	4.80±0.75†	3.40±0.80†		
deer-truck	4.80±1.17	4.80±1.17	5.00±0.89	4.60±1.02†	5.20±0.75	5.20±1.33†	4.60±0.80†	4.20±0.80†		
deer-horse	4.00±0.63	4.40±0.80†	5.20±1.17†	3.40±0.80	5.00±0.00†	5.00±0.00†	5.00±0.63†	5.20±0.75†		
automobile-truck	4.40±1.02	4.20±1.47	4.40±0.80†	3.20±1.33	5.00±1.41†	5.00±1.26†	5.20±0.40	4.80±0.75		
cat-dog	4.00±1.10	4.00±1.26	4.00±1.26	4.40±1.50†	3.40±0.49†	5.40±0.80	4.60±1.02	3.60±0.49†		
dog-horse	4.00±1.10	5.00±0.89	5.40±1.02	5.00±0.63	4.60±0.80	5.00±0.63†	4.20±0.75	5.40±0.80		
t-test (W/T/L)	—	2/8/2	3/7/2	3/8/1	3/6/3	5/6/1	1/7/4	3/4/5		
Average Rank	3.96	4.79	6.00	4.00	5.38	5.38	3.25	3.25		

(b) Comparison on the *size of the (sub-)ensemble architectures*.

Label Pair				Time Cost (min)						
	AdaNet	PRS	PAP	PIE	AdaNet.W	PRS.W	PAP.W	PIE.W		
digits 6-9	10.92±1.82	12.35±0.99	12.91±1.31	13.04±0.76	12.74±1.29	12.24±0.92	13.50±0.28	12.61±1.84†		
digits 5-8	13.00±0.46	12.25±0.64†	13.96±0.34†	12.16±0.49†	13.07±0.46†	13.07±0.83†	13.16±0.62†	13.55±1.18†		
top-pullover	11.83±0.46	11.93±0.52†	12.78±1.29†	11.73±1.77	11.84±0.98†	11.22±1.01	12.08±0.58†	11.02±0.28†		
top-coat	12.00±0.68	11.21±0.34†	11.05±0.70	11.78±1.27	12.42±0.52	11.90±0.67†	12.04±0.62	11.09±0.17†		
top-shirt	11.80±1.06	12.06±1.18†	12.63±0.85	10.89±2.53	12.55±0.66	12.63±0.74	12.04±0.83	12.26±1.34†		
trouser-dress	10.88±1.40	11.98±0.61	12.36±1.02†	11.24±1.74†	12.19±0.66	10.75±1.72	11.92±0.71	12.25±1.23		
sandal-ankle boot	11.75±0.94	12.09±0.99†	12.55±1.04†	10.20±2.35	13.03±0.40	12.34±0.47	12.20±0.77	11.34±0.91†		
deer-truck	15.50±1.81	13.32±2.08	11.72±1.01†	11.39±0.81†	16.74±1.00	16.11±1.24	16.90±0.90	15.51±1.18		
deer-horse	14.66±1.09	12.70±0.98†	11.94±1.08†	9.82±0.58†	16.22±0.68	15.99±1.08	16.94±1.04	17.12±1.03†		
automobile-truck	15.31±1.33	12.64±2.23	11.35±1.15†	10.04±1.31†	15.87±1.70†	16.42±1.36†	16.52±0.50	16.97±0.89		
cat-dog	24.28±17.37	17.17±1.48†	23.06±11.87†	75.08±113.67†	14.45±1.29†	78.41±104.25†	113.55±193.13†	35.34±38.05†		
dog-horse	16.79±2.68	23.08±12.98†	77.02±116.93†	16.07±1.02†	71.94±108.17†	119.54±189.82†	17.00±1.81	46.69±39.39†		
t-test (W/T/L)	—	4/4/4	5/3/4	2/5/5	4/7/1	4/7/1	3/9/0	6/3/3		
Average Rank	3.25	3.50	5.17	2.50	5.58	5.00	6.08	4.92		

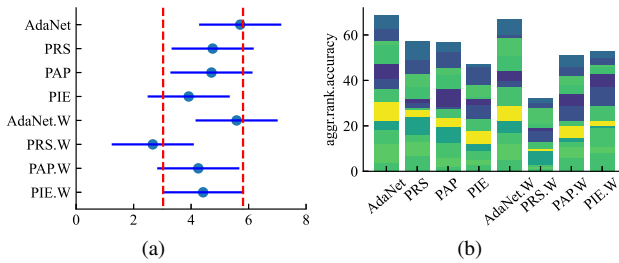
(c) Comparison on the *time cost (min)* of the searching process.

Fig. 2. Comparison of the baseline AdaNet and the proposed SAEP including their variants on the *test accuracy*, using MLPs as sub-architectures for binary classification. (a) Friedman test chart (non-overlapping means significant difference) [27], which rejects the assumption that “all methods have the same accuracy performance” at the significance level of 10%. (b) The aggregated rank of test accuracy for each method (the smaller the better) [32].

coats, sandals, shirts, sneakers, bags, and ankle boots, respectively.

B. Baseline Methods

To analyze the effectiveness of SAEP, we compare the three proposed solutions (i.e., PRS, PAP, and PIE) with AdaNet [5].

Besides, AdaNet (usually set to use uniform average weights in practice) has a variant to use mixture weights, which we call AdaNet.W [33]. Similarly, PRS.W, PAP.W, and PIE.W (i.e., SAEP.W) are variants of PRS, PAP, and PIE using mixture weights, respectively. Our baselines include AdaNet and their corresponding variants. Besides, to objectively evaluate the performance of these methods, standard 5-fold cross-validation is used in these experiments, i.e., in each iteration, the entire data set is split into two parts, with 80% as the training set and 20% as the test set.

C. Experimental Settings

In the same experiment, all methods would use the same kind of sub-architectures in consideration of fairness during the comparisons to verify whether their objectives work well. The optional sub-architectures that we use include multi-layer perceptrons (MLPs) and convolutional neural networks (CNNs). Note that those CNNs are only composed of convolution layers with 16 channels, without pooling layers. As for the hyper-parameters in the experiments, the learning rate is set to be 0.003, and cosine decay is applied to the learning

TABLE III

EMPIRICAL RESULTS OF ENSEMBLE-ARCHITECTURES' PERFORMANCE FOR MULTI-CLASS CLASSIFICATION. EACH METHOD INCLUDES FOUR COLUMNS, I.E., THE *test accuracy (%)*, THE *size* OF GENERATED (SUB-)ENSEMBLE ARCHITECTURES, THE *diversity* OF THE PRUNED SUB-ENSEMBLE ARCHITECTURES, AND THE *time cost (min)* OF THE SEARCHING PROCESS. THE BEST OF THEM ARE INDICATED WITH BOLD FONTS FOR EACH DATASET (ROW). NOTE THAT SUB-ARCHITECTURES USED IN THESE EXPERIMENTS ARE MLPs AND CNNs.

Dataset	Test Accuracy (%)							
	AdaNet	PRS	PAP	PIE	AdaNet.W	PRS.W	PAP.W	PIE.W
MNIST	94.88±0.22	94.82±0.36†	94.79±0.23†	94.75±0.25†	94.94±0.29	94.66±0.13	94.56±0.28†	94.94±0.19†
Fashion-MNIST	83.74±0.52	83.76±0.88	83.95±0.50†	83.89±0.64	83.81±0.32†	83.98±0.40†	84.24±0.18†	83.93±0.21†
MNIST*	90.54±0.24	90.46±0.25†	90.44±0.15	90.35±0.24†	90.55±0.18†	90.38±0.27†	90.27±0.16	90.23±0.35†
Fashion-MNIST*	81.39±0.43	81.48±0.30†	81.40±0.23†	81.32±0.45†	81.39±0.26†	81.41±0.18†	81.20±0.09	81.05±0.58†
t-test (W/T/L)	—	2/1/1	1/1/2	3/1/0	0/1/3	1/1/2	1/2/1	2/0/2
Average Rank	4.50	3.75	3.75	5.75	3.25	4.00	5.75	5.25
Dataset	Number of Sub-Architectures							
	AdaNet	PRS	PAP	PIE	AdaNet.W	PRS.W	PAP.W	PIE.W
MNIST	6.80±0.40	6.60±0.49	7.00±0.00	6.60±0.49	6.60±0.49	6.20±0.98	5.20±0.75†	6.80±0.40
Fashion-MNIST	5.40±1.02	5.60±0.80	5.40±1.02	6.00±0.63	6.00±0.89	5.60±0.80	5.00±0.63†	4.00±1.10
MNIST*	5.80±0.75	4.80±0.75†	5.60±1.50	4.80±0.40†	5.40±1.36	5.00±1.41	3.80±1.17	3.00±0.00†
Fashion-MNIST*	5.40±1.36	3.80±1.47†	6.40±0.49	5.00±0.63†	5.60±0.49	4.00±0.63†	4.00±0.89†	3.20±0.40†
t-test (W/T/L)	—	0/2/2	0/4/0	0/2/2	0/4/0	0/3/1	0/1/3	0/2/2
Average Rank	6.00	3.75	6.63	5.00	6.13	4.00	2.13	2.38
Dataset	Time Cost (min)							
	AdaNet	PRS	PAP	PIE	AdaNet.W	PRS.W	PAP.W	PIE.W
MNIST	78.65±89.02	23.42±2.32†	21.51±0.16†	31.73±12.46†	81.13±87.66	43.36±12.72†	92.39±117.81†	33.11±1.94†
Fashion-MNIST	21.75±1.87	20.07±0.65†	25.50±9.07†	39.30±6.03†	42.92±9.71†	91.41±117.32†	31.77±2.16†	75.92±89.19†
MNIST*	30.73±1.10	29.03±0.74†	28.04±3.87	20.47±1.27†	30.46±1.72	25.88±2.62†	29.08±1.23	28.25±0.08†
Fashion-MNIST*	29.61±1.53	27.74±1.75†	30.63±1.53†	20.90±0.83†	31.12±0.57†	25.01±3.19	28.22±1.92	28.28±0.19†
t-test (W/T/L)	—	0/0/4	2/1/1	1/0/3	2/2/0	1/1/2	2/2/0	1/0/3
Average Rank	5.50	2.75	3.50	2.50	7.00	4.25	5.50	5.00

¹ Empirical results with * represent experiments using CNNs as sub-architectures; Empirical results without * represent experiments using MLPs as sub-architectures.

² The reported results are the average values of each method and the corresponding standard deviation under 5-fold cross-validation on each dataset.

³ By two-tailed paired *t*-test at 5% significance level, † and ‡ denote that the performance of AdaNet is inferior to and superior to that of the comparative SAEP method with their variants, respectively.

⁴ The last two rows show the results of *t*-test and average rank, respectively. The "W/T/L" in *t*-test indicates that AdaNet is superior to, not significantly different from, or inferior to the corresponding comparative SAEP methods including their variants. The average rank is calculated according to the Friedman test [27].

rate using a momentum optimizer in the training process. The number of training steps is 5,000, and that of the batch size is 64.

We use three datasets mentioned before for image classification. In the multi-class classification scenario, we use all of the categories in the corresponding dataset; in the binary classification scenario, we reduce these datasets by considering several pairs of classes. For example, we consider five pairs of classes in CIFAR-10 (i.e., deer-truck, deer-horse, automobile-truck, cat-dog, and dog-horse), five pairs of classes in Fashion-MNIST (i.e., top-pullover, top-coat, top-shirt, trouser-dress, and sandal-ankle boot), and two pairs of digits in MNIST (i.e., digits 6-9, and 5-8).

D. SAEP Could Achieve Ensemble Architectures with Better Performance of Accuracy

In this subsection, we verify whether the pruned sub-ensemble architectures could achieve comparable performance with the original ensemble architecture. Experimental results are reported in Tables II–III contain the average test accuracy (%) of each method and the corresponding standard deviation under 5-fold cross-validation on each data set. For instance, each row (data set) in Table II compares the classification accuracy using sub-architectures with the same type, indicating results with higher accuracy and lower standard deviation by bold fonts. When comparing one method with AdaNet, the one with higher values of accuracy and lower standard deviation would win; otherwise, the winner would be decided based on the significance of the difference in the accuracy performance between the two methods, which is examined by two-tailed paired *t*-test at 5% significance level to tell if two methods have significantly different results. Specifically, two

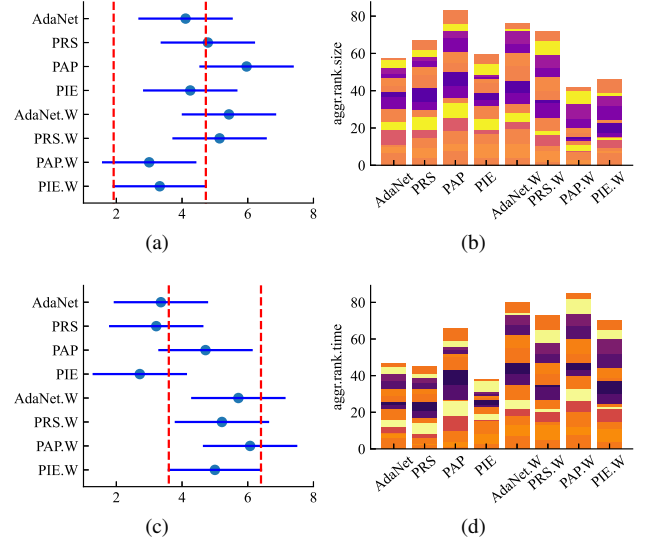


Fig. 3. Comparison of the baseline AdaNet and the proposed SAEP including their variants, using MLPs as sub-architectures for image classification. (a–b) Comparison on the *size* of generated (sub-)ensemble architectures. (c–d) Comparison on the *time cost* of the searching process. Notice that: the Friedman test chart in (a) rejects the assumption that “the size of ensemble architectures of different methods has no significant difference” at 5% significant level; that in (c) rejects the assumption that “the time cost of different methods has no significant difference” at 5% significant level.

methods end up with a tie if there is no significant statistical difference between them; otherwise, the one with higher values of accuracy would win. The performance of each method is reported in the last two rows of Table II, compared with AdaNet in terms of the average rank and the number of data sets that AdaNet has won, tied, or lost, respectively. We may notice that SAEP achieved better results than AdaNet in most cases, yet with possible larger time cost in a few cases. Therefore, it could be referred that SAEP could generate ensemble architectures with better performance of accuracy. Figure 2(a) shows that SAEP (indicated by PRS, PAP, and PIE) achieves the same level of accuracy performance as AdaNet at least, and their variants even exhibits better accuracy performance than AdaNet and AdaNet.W. Similar results are presented in Figure 2(b) and Table III.

E. SAEP Leads to Ensemble Architectures with Smaller Size

In this subsection, we verify whether the pruned sub-ensemble architectures could generate comparable performance of architectures with smaller size. Experimental results are reported in Tables II–III and Figures 3–4. As we can see in Table II, SAEP achieves ensemble architectures with the smallest size in most cases, although the significant difference between different methods might not be as large as that of accuracy, as shown in Figures 3(a)–3(b). Meanwhile, Table II and Figures 3(c)–3(d) presents that variants of AdaNet and SAEP might cost more time than themselves. However, considering that SAEP already achieves the comparable performance with AdaNet and that SAEP generates ensemble architectures with smaller size indeed, we believe that our NAS ensemble pruning method is still meaningful somehow. Similar observations are

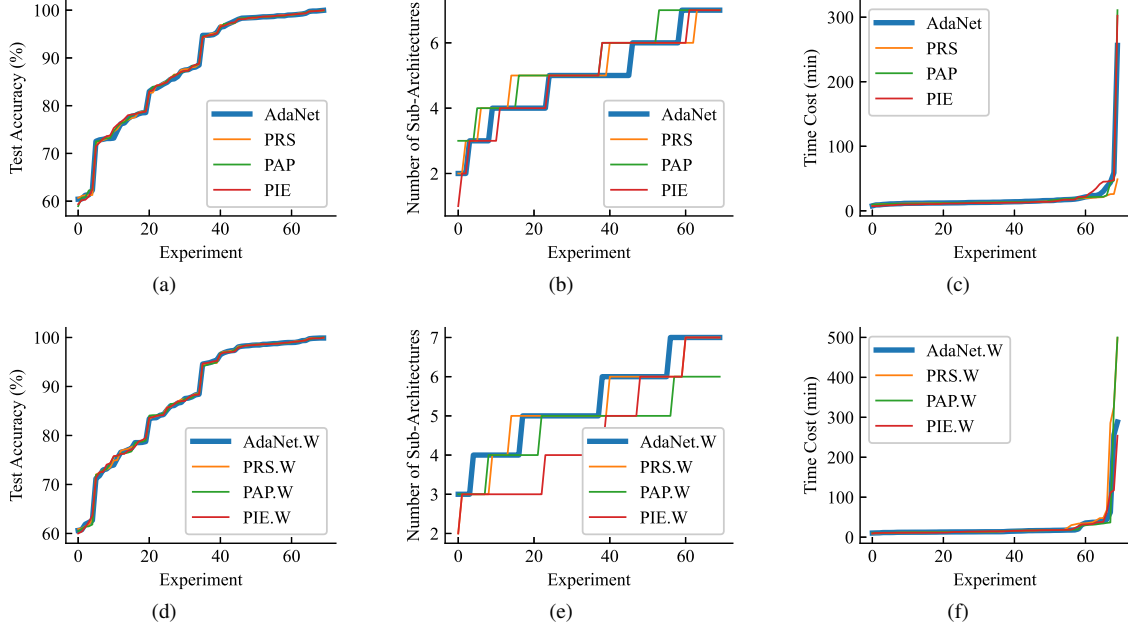


Fig. 4. Comparison of the baseline AdaNet and the proposed *SAEP* including their corresponding variants, using MLPs as sub-architectures for image classification. The horizontal axis represents empirical results in different specific experiments like different rows in Tables II–III. (a–c) Comparison of performance of AdaNet and *SAEP*. (d–f) Comparison of performance of their corresponding variants.

exhibited in Figure 4 as well: (1) *SAEP* could achieve the same level of accuracy performance as AdaNet, as shown in Figures 4(a) and 4(d); (2) *SAEP* could generate ensemble architectures with competitive performance yet smaller size, as shown in Figure 4(e).

F. *PIE* Generates Sub-Ensemble Architectures with More Diversity

In this subsection, we verify whether the purpose of increasing the diversity of ensemble architectures is satisfied. We use the normalized of information VI in *PIE* to imply the redundancy between two different sub-architectures, indicating the diversity between them. However, in this experiment, we use another measure named the disagreement measure [34], [35] here to calculate the diversity for the ensemble architecture and the pruned sub-ensemble architectures, because there is no analogous term like VI in *PRS* and *PAP*. Note that researchers proposed many other measures to calculate diversity, and the disagreement measure is one of them [36]. We choose the disagreement measure here because this measure is easy to be calculated and understood. The disagreement between two sub-architectures \mathbf{w}_i and \mathbf{w}_j is

$$\text{dis}(\mathbf{w}_i, \mathbf{w}_j) = \frac{1}{m} \sum_{1 \leq i \leq m} \mathbb{I}(\mathbf{h}_i(\mathbf{x}_i) \neq \mathbf{h}_j(\mathbf{x}_i)), \quad (17)$$

the diversity of the ensemble architecture f using the disagreement measure is

$$\text{dis}(f) = \frac{2}{l(l-1)} \sum_{\mathbf{w}_i \cdot \mathbf{h}_i \in f} \sum_{\substack{\mathbf{w}_j \cdot \mathbf{h}_j \in f, \\ \mathbf{h}_j \neq \mathbf{h}_i}} \text{dis}(\mathbf{w}_i, \mathbf{w}_j), \quad (18)$$

and the diversity of the sub-ensemble architecture $f \setminus \{\mathbf{w} \cdot \mathbf{h}\}$ could be calculated analogously.

Table IV and Figures 5–6 report their performance with the corresponding disagreement value reflecting the diversity of the whole ensemble architecture as well. Besides, Table IV reports the diversity of the sub-architectures using *PIE* and other corresponding information. Note that the larger the disagreement is, the larger the diversity of the ensemble architecture or the pruned sub-architecture is. *PAP* in Table IV achieves better accuracy performance and more diversity concurrently. Similar results are observed in *PRS.W* and *PAP.W* compared with *AdaNet.W* in Table IV, which illustrates that the accuracy of the sub-ensemble architecture could benefit from increasing diversity. Meanwhile, Table IV shows that larger sub-ensemble architectures correspond to less diversity sometimes. In addition, Figure 6 indicate the effect of the α value in Eq. (15) on the diversity, the accuracy performance, the time cost, and the size of the sub-ensemble architectures.

G. Effect of the α Value

This subsection will investigate the effect of the hyper-parameter α in *PIE*. The value of α indicates the relation between two criteria in Eq. (15) as well. To reveal this issue, different α values (from 0.0 to 1.0 with 0.05 steps) are evaluated in the experiments. Figure 6 exemplify the effect of α on the MNIST dataset, taking the label pairs of digits 5-8 and digits 6-9 as an example. Figure 6(a) illustrates that the accuracy of sub-ensemble architectures is affected slightly under different α values yet would not cause much accuracy decline. Figure 6(b) illustrates that the diversity of the sub-ensemble architectures in *PIE.W* is affected under different α values yet without large changes of absolute values; meanwhile, the diversity of that in *PIE* is almost not affected under different α values. Figures 6(c)–6(d) present that the

TABLE IV

EMPIRICAL RESULTS UNDER DIFFERENT α VALUES ON THE MNIST DATASET FOR BINARY CLASSIFICATION (TO BE SPECIFIC, THE LABEL PAIR OF DIGITS 5 – 8), USING MLPs AS SUB-ARCHITECTURES. EACH METHOD INCLUDES FOUR COLUMNS: THE *test accuracy (%)*, THE *diversity (disagreement)*, THE *size* (I.E., THE NUMBER OF SUB-ARCHITECTURES), AND THE *time cost (min)* OF THE SEARCHING PROCESS. NOTE THAT “ORIG.” REPRESENTS ADANET, PRS, PAP, OR PIE; “VARI.” REPRESENTS ADANET.W, PRS.W, PAP.W, OR PIE.W, CORRESPONDINGLY.

	Test Accuracy (%)		Diversity (Disagreement)		Size		Time Cost (min)	
	orig.	vari.	orig.	vari.	orig.	vari.	orig.	vari.
AdaNet	99.86±0.06	99.86±0.05	0.0003±0.0001	0.0005±0.0003	5.60±5.60	5.80±5.80	11.53±0.43	12.37±0.75
PRS	99.83±0.07	99.88±0.05	0.0037±0.0043	0.0019±0.0031	5.40±5.40	4.80±4.80	11.93±0.71	11.16±1.52
PAP	99.87±0.05	99.88±0.04	0.0011±0.0018	0.0003±0.0001	5.80±5.80	5.40±5.40	12.76±1.06	12.89±0.62
PIE ($\alpha = 0.5$)	99.80±0.06	99.85±0.04	0.0037±0.0069	0.0030±0.0053	4.80±4.80	5.80±5.80	12.29±1.14	13.15±0.54
PIE ($\alpha = 0.0$)	99.15±0.23	99.19±0.26	0.0022±0.0004	0.0399±0.0201	7.00±0.00	5.80±0.40	14.53±0.10	13.98±0.63
PIE ($\alpha = 0.05$)	99.16±0.24	99.16±0.13	0.0024±0.0004	0.0280±0.0135	6.60±0.80	6.00±1.10	9.56±2.14	13.60±1.16
PIE ($\alpha = 0.1$)	99.13±0.04	99.21±0.15	0.0019±0.0003	0.0456±0.0250	6.40±0.49	5.40±1.20	13.59±0.80	13.22±0.91
PIE ($\alpha = 0.15$)	99.24±0.14	99.25±0.17	0.0020±0.0004	0.0313±0.0299	6.00±0.89	5.80±0.98	12.95±0.64	14.00±0.75
PIE ($\alpha = 0.2$)	99.14±0.17	99.21±0.06	0.0022±0.0006	0.0574±0.0162	6.20±0.75	6.40±0.49	14.20±0.72	14.58±0.18
PIE ($\alpha = 0.25$)	99.22±0.12	99.15±0.19	0.0020±0.0004	0.0378±0.0294	6.00±0.63	6.40±0.80	13.08±0.61	14.30±0.71
PIE ($\alpha = 0.3$)	99.29±0.12	99.18±0.22	0.0023±0.0003	0.0415±0.0251	7.00±0.00	6.40±0.49	13.16±1.54	14.36±0.41
PIE ($\alpha = 0.35$)	99.19±0.11	99.24±0.09	0.0021±0.0006	0.0210±0.0158	5.60±1.02	5.40±1.20	12.85±0.73	13.20±0.93
PIE ($\alpha = 0.4$)	99.22±0.13	99.20±0.22	0.0022±0.0002	0.0364±0.0288	6.80±0.40	6.20±0.75	11.02±0.12	14.49±0.53
PIE ($\alpha = 0.45$)	99.12±0.12	99.18±0.18	0.0023±0.0009	0.0486±0.0232	6.60±0.80	6.60±0.80	13.62±0.40	14.59±0.44
PIE ($\alpha = 0.55$)	99.17±0.19	99.18±0.20	0.0022±0.0004	0.0454±0.0107	6.00±0.63	6.40±0.49	12.99±0.69	14.45±0.59
PIE ($\alpha = 0.6$)	99.23±0.08	99.19±0.15	0.0022±0.0002	0.0499±0.0275	6.00±1.10	5.60±0.80	9.96±1.46	13.65±1.03
PIE ($\alpha = 0.65$)	99.20±0.14	99.29±0.12	0.0018±0.0003	0.0173±0.0147	6.40±0.80	5.40±1.02	13.14±0.87	13.21±1.08
PIE ($\alpha = 0.7$)	99.23±0.21	99.25±0.12	0.0020±0.0003	0.0234±0.0228	6.60±0.80	6.00±1.26	8.17±0.64	13.78±0.83
PIE ($\alpha = 0.75$)	99.16±0.21	99.22±0.15	0.0022±0.0005	0.0428±0.0216	6.60±0.49	6.00±0.63	13.48±0.51	14.21±0.64
PIE ($\alpha = 0.8$)	99.17±0.15	99.19±0.03	0.0028±0.0017	0.0269±0.0213	6.40±0.49	5.40±1.20	7.80±0.47	13.35±1.05
PIE ($\alpha = 0.85$)	99.20±0.13	99.18±0.17	0.0020±0.0003	0.0411±0.0224	5.60±0.49	6.60±0.49	12.81±0.35	14.45±0.47
PIE ($\alpha = 0.9$)	99.20±0.23	99.28±0.16	0.0017±0.0003	0.0596±0.0172	6.00±0.63	6.00±0.63	7.67±0.92	13.99±0.45
PIE ($\alpha = 0.95$)	99.22±0.19	99.22±0.10	0.0020±0.0003	0.0283±0.0210	5.80±0.40	5.80±1.17	12.51±0.38	13.82±0.80
PIE ($\alpha = 1.0$)	99.19±0.19	99.28±0.15	0.0021±0.0006	0.0483±0.0159	6.20±0.75	6.40±0.49	8.07±0.35	14.34±0.27

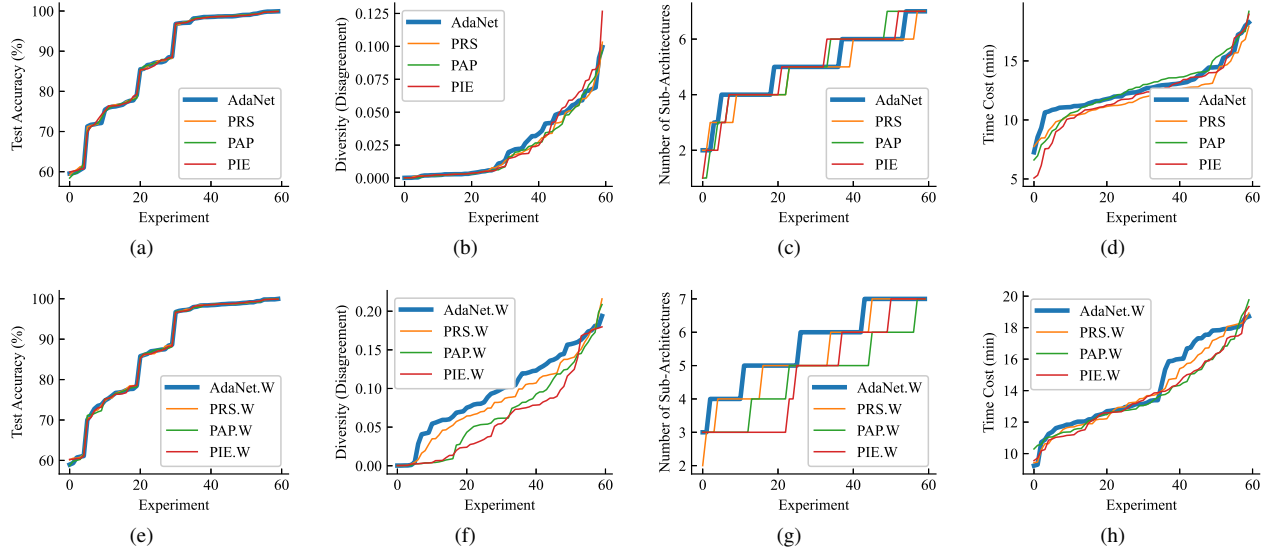


Fig. 5. Comparison of the baseline AdaNet and the proposed SAEP including their corresponding variants, using MLPs as sub-architectures for binary classification. The horizontal axis represents empirical results in different specific experiments like different rows in Tables II–III. (a–c) Comparison of performance of AdaNet and SAEP. (d–f) Comparison of performance of their corresponding variants.

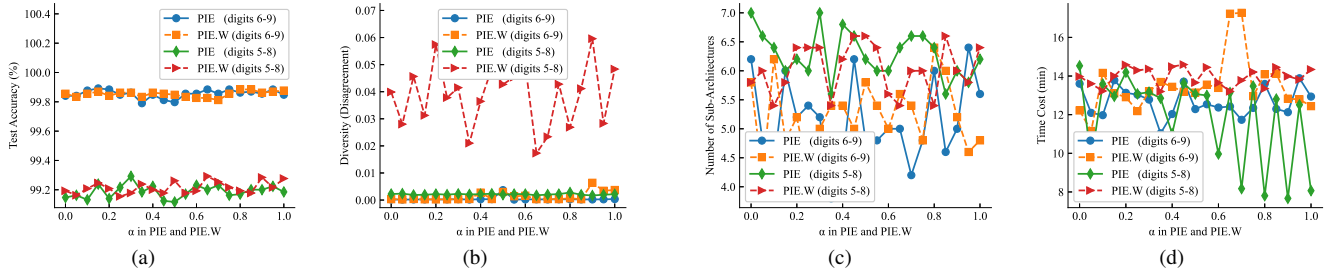


Fig. 6. The effect of different α values in *PIE* and *PIE.W* for binary classification. (a) The effect of the α value on the test accuracy performance of sub-ensemble architectures. (b) The effect of the α value on the diversity of sub-ensemble architectures, measured by the disagreement measure in Eq. (18). (c) The effect of the α value on the size of sub-ensemble architectures. (d) The effect of the α value on the time cost.

TABLE V

EMPIRICAL RESULTS OF THE EXACT SUB-ARCHITECTURES THAT ARE KEPT IN THE FINAL SUB-ENSEMBLE ARCHITECTURE AFTER PRUNING ON THE DIGITS 5-8 LABEL PAIR IN THE MNIST DATASET. EACH METHOD INCLUDES FIVE COLUMNS: THE *test accuracy (%)*, THE *diversity (disagreement)*, THE *time cost (min)*, THE *size* (I.E., THE NUMBER OF SUB-ARCHITECTURES), AND THE *indexes* OF THE GENERATED SUB-ARCHITECTURES. NOTE THAT THE SUB-ARCHITECTURES USED IN THESE EXPERIMENTS ARE MLPs.

	Accuracy	Diversity	Time	Size	Indexes
AdaNet	99.86	0.0001	10.71	6	[0,1,3,4,5,6]
PRS	99.92	0.0101	10.54	4	[0,1,2,5]
PAP	99.93	0.0002	13.95	7	[0,1,2,3,4,5,6]
PIE ($\alpha=0.25$)	99.24	0.0016	13.31	6	[0,1,2,3,4,5]
PIE ($\alpha=0.5$)	99.89	0.0002	12.89	5	[0,1,2,3,4]
PIE ($\alpha=0.75$)	99.12	0.0024	13.53	6	[0,1,2,3,5,6]
AdaNet.W	99.82	0.0002	11.69	5	[0,1,2,3,6]
PRS.W	99.93	0.0006	13.82	7	[0,1,2,3,4,5,6]
PAP.W	99.86	0.0003	12.47	6	[0,1,3,4,5,6]
PIE.W ($\alpha=0.25$)	99.20	0.0029	12.91	5	[0,1,2,3,6]
PIE.W ($\alpha=0.5$)	99.78	0.0004	13.69	6	[0,1,2,3,4,5]
PIE.W ($\alpha=0.75$)	99.01	0.0445	13.99	6	[0,1,2,3,4,6]

size and time cost of sub-ensemble architectures would be more affected under different α values. Generally, the size and time cost of sub-ensemble architectures in *PIE* tend to be decreased with the increase of α value.

H. AdaNet v.s. SAEP over the Time Cost

In this subsection, we compare the time cost of AdaNet and SAEP with their corresponding variants. Experimental results are reported in Tables II–IV and Figures 3–6, containing the accuracy on the test set of each method and their corresponding time cost. Although Figures 3(c)–3(d) illustrate that the time cost is not an advantage of SAEP compared with AdaNet while achieving the same level of accuracy, Tables II–III present that SAEP could generate satisfactory sub-ensemble architectures within less time sometimes. Generally, the time cost depends on the number of sub-architectures that are generated during the entire searching process, although the pruning is proceeded through the same process. Therefore, it is quite understandable that SAEP might take a longer time if more sub-architectures are generated during searching. Moreover, Figure 6(d) presents the effect of different α values in *PIE* on the time cost of generating sub-ensemble architectures with more diversity.

I. SAEP Could Generate Distinct Deeper Sub-Architectures than AdaNet

In a few cases, we observe that *PIE* could achieve a larger ensemble architecture than AdaNet, which makes us wonder whether SAEP could lead to distinct architectures from AdaNet. Thus, we dig the sub-architectures that are kept in the final architecture to explore more details deep down inside. As we can see in Table V, the size of sub-ensemble architectures tends to be larger under the lower level of diversity. The reason why *PIE* (or *PIE.W*) generates distinct deeper sub-architectures might be the diversity is not sufficient for its objective in Eq. (16). In this case, the objective would guide the pruning process to search for more distinct deeper sub-architectures to increase diversity.

V. RELATED WORK

In this section, we introduce the neural architecture search (NAS) briefly. The concept of “neural architecture search (NAS)” was proposed by Zoph and Le [4] for the very first time. They presented NAS as a gradient-based method to find good architectures. A “controller”, denoted by a recurrent network, was used to generate variable-length string which specified the structure and connectivity of a neural network; the generated “child network,” specified by the string, was then trained on the real data to obtain accuracy as the reward signal, to generate an architecture with higher probabilities to receive high accuracy [1], [4], [37]. Existing NAS methods could be categorized under three dimensions: search space, search strategy, and performance estimation strategy [2], [38]–[40]. Classical NAS methods yielded chain-structured neural architectures [2], [41], yet ignored some modern designed elements from hand-crafted architectures, such as skip connections from ResNet [42]. Thus some researchers also attempted to build complex multi-branch networks by incorporating those and achieved positive results [43]–[50].

Recently, NAS methods involved ensemble learning are attracting researchers’ attention gradually. Cortes *et al.* [5] proposed a data-dependent learning guarantee to guide the choice of additional sub-networks and presented AdaNet to learn neural networks adaptively. They claimed that AdaNet could precisely address some of the issues of wasteful data, time, and resources in neural architecture search since their optimization problem for AdaNet was convex and admitted a unique global solution. Besides, Huang *et al.* [6] specialized sub-architectures by residual blocks and claimed that their BoostResNet boosted over multi-channel representations/features, which was different from AdaNet. Macko *et al.* [7] also proposed another attempt named as AdaNAS to utilize ensemble methods to compose a neural network automatically, which was an extension of AdaNet with the difference of using subnetworks comprising stacked NASNet [1], [4] blocks. However, both of them gathered all searched sub-architectures together and missed out on the critical characteristic that ensemble models usually benefit from diverse individual learners.

Moreover, Chang *et al.* [51] proposed Differentiable Architecture Search with Ensemble Gumbel-Softmax (DARTS-EGS) and developed ensemble Gumbel-Softmax to maintain efficiency in searching. Ardywibowo *et al.* [52] constructed an ensemble model to perform the Out-of-Distribution (OOD) detection in their Neural Architecture Distribution Search (NADS), which searched for a distribution of architectures instead of one single best-performing architecture in standard neural architecture search methods. These two methods are not discussed in this paper since they are not assembling sub-architectures during searching.

VI. CONCLUSION

Recent attempts on NAS with ensemble learning methods have achieved prominent results in reducing the search complexity and improving the effectiveness [5]. However, current approaches usually miss out on an essential characteristic

of diversity in ensemble learning. To tackle this problem, in this paper, we target the ensemble learning methods in NAS and propose an ensemble pruning method named “*Sub-Architecture Ensemble Pruning in Neural Architecture Search (SAEP)*” to reduce the redundant sub-architectures during the searching process. Three solutions are proposed as the guiding criteria in *SAEP* that reflect the characteristics of the ensemble architecture (i.e., *PRS*, *PAP*, and *PIE*) to prune the less valuable sub-architectures. Experimental results indicate that *SAEP* could guide diverse sub-architectures to create sub-ensemble architectures in a smaller size yet still with comparable performance to the ensemble architecture that is not pruned. Besides, *PIE* might lead to distinct deeper sub-architectures if diversity is insufficient. In the future, we plan to generalize the current method to more diverse ensemble strategies and derive theoretical guarantees to further improve the performance of the NAS ensemble architectures.

REFERENCES

- [1] B. Zoph, V. Vasudevan, J. Shlens, and Q. Le, “Learning transferable architectures for scalable image recognition,” in *CVPR*, 2018, pp. 8697–8710.
- [2] T. Elsken, J. H. Metzen, and F. Hutter, “Neural architecture search,” in *Automated Machine Learning*. Springer, 2019, pp. 63–77.
- [3] M. Wistuba, A. Rawat, and T. Pedapati, “A survey on neural architecture search,” *arXiv preprint arXiv:1905.01392*, 2019.
- [4] B. Zoph and Q. Le, “Neural architecture search with reinforcement learning,” in *ICLR*, 2017.
- [5] C. Cortes, X. Gonzalvo, V. Kuznetsov, M. Mohri, and S. Yang, “Adanet: Adaptive structural learning of artificial neural networks,” in *ICML*, 2017, pp. 874–883.
- [6] F. Huang, J. Ash, J. Langford, and R. Schapire, “Learning deep resnet blocks sequentially using boosting theory,” in *ICML*, 2018.
- [7] V. Macko, C. Weill, H. Mazzawi, and J. Gonzalvo, “Improving neural architecture search image classifiers via ensemble learning,” *arXiv preprint arXiv:1903.06236*, 2019.
- [8] C. Cortes, M. Mohri, and U. Syed, “Deep boosting,” in *ICML*, 2014, pp. 1179–1187.
- [9] H. Chen and X. Yao, “Regularized negative correlation learning for neural network ensembles,” *IEEE T Neural Networ*, vol. 20, no. 12, pp. 1962–1979, 2009.
- [10] —, “Multiobjective neural network ensembles based on regularized negative correlation learning,” *IEEE T Knowl Data En*, vol. 22, no. 12, pp. 1738–1751, 2010.
- [11] —, “Evolutionary random neural ensembles based on negative correlation learning,” in *IEEE CEC*. IEEE, 2007, pp. 1468–1474.
- [12] Y. Bian, Y. Wang, Y. Yao, and H. Chen, “Ensemble pruning based on objection maximization with a general distributed framework,” *IEEE T Neur Net Lear*, vol. 31, no. 9, pp. 3766–3774, 2020.
- [13] H. Chen, P. Tino, and X. Yao, “A probabilistic ensemble pruning algorithm,” in *ICDM Workshops*. IEEE, 2006, pp. 878–882.
- [14] H. Chen, P. Tiño, and X. Yao, “Predictive ensemble pruning by expectation propagation,” *IEEE T Neural Networ*, vol. 21, no. 7, pp. 999–1013, 2009.
- [15] H. Chen, “Diversity and regularization in neural network ensembles,” Ph.D. dissertation, University of Birmingham, 2008.
- [16] Y. Bian and H. Chen, “When does diversity help generalization in classification ensembles?” *IEEE Trans. Cybern.*, pp. 1–17, 2021.
- [17] Z. Lu, X. Wu, X. Zhu, and J. Bongard, “Ensemble pruning via individual contribution ordering,” in *SIGKDD*. ACM, 2010, pp. 871–880.
- [18] N. Li, Y. Yu, and Z.-H. Zhou, “Diversity regularized ensemble pruning,” in *ECML-PKDD*, 2012, pp. 330–345.
- [19] G. Martínez-Muñoz and A. Suárez, “Using boosting to prune bagging ensembles,” *Pattern Recogn Lett*, vol. 28, no. 1, pp. 156–165, 2007.
- [20] K. Jarrett, K. Kavukcuoglu, M. Ranzato, and Y. LeCun, “What is the best multi-stage architecture for object recognition?” in *ICCV*. IEEE, 2009, pp. 2146–2153.
- [21] V. Nair and G. Hinton, “Rectified linear units improve restricted boltzmann machines,” in *ICML*, 2010, pp. 807–814.
- [22] X. Glorot, A. Bordes, and Y. Bengio, “Deep sparse rectifier neural networks,” in *AISTATS*, 2011, pp. 315–323.
- [23] I. Goodfellow, Y. Bengio, A. Courville, and Y. Bengio, *Deep Learning*. MIT press Cambridge, 2016, vol. 1.
- [24] V. Koltchinskii, D. Panchenko *et al.*, “Empirical margin distributions and bounding the generalization error of combined classifiers,” *Ann Stat*, vol. 30, no. 1, pp. 1–50, 2002.
- [25] S. Zadeh, M. Ghadiri, V. Mirrokni, and M. Zadimoghaddam, “Scalable feature selection via distributed diversity maximization,” in *AAAI*, 2017, pp. 2876–2883.
- [26] T. Cover and J. Thomas, *Elements of information theory*. John Wiley & Sons, 2012.
- [27] J. Demšar, “Statistical comparisons of classifiers over multiple data sets,” *J Mach Learn Res*, vol. 7, no. Jan, pp. 1–30, 2006.
- [28] J. Deng, W. Dong, R. Socher, L.-J. Li, K. Li, and L. Fei-Fei, “Imagenet: A large-scale hierarchical image database,” in *CVPR*. IEEE, 2009, pp. 248–255.
- [29] A. Krizhevsky and G. Hinton, “Learning multiple layers of features from tiny images,” Citeseer, Tech. Rep., 2009.
- [30] Y. LeCun, L. Bottou, Y. Bengio, and P. Haffner, “Gradient-based learning applied to document recognition,” *Proceedings of the IEEE*, vol. 86, no. 11, pp. 2278–2324, 1998.
- [31] H. Xiao, K. Rasul, and R. Vollgraf, “Fashion-mnist: a novel image dataset for benchmarking machine learning algorithms,” *arXiv preprint arXiv:1708.07747*, 2017.
- [32] C. Qian, Y. Yu, and Z.-H. Zhou, “Pareto ensemble pruning,” in *AAAI*, 2015, pp. 2935–2941.
- [33] C. Weill, J. Gonzalvo, V. Kuznetsov, S. Yang, S. Yak, H. Mazzawi, E. Hotaj, G. Jerfel, V. Macko, M. Mohri, and C. Cortes, “Adanet: Fast and flexible automl with learning guarantees,” 2018. [Online]. Available: <https://github.com/tensorflow/adanet>
- [34] D. B. Skalak *et al.*, “The sources of increased accuracy for two proposed boosting algorithms,” in *AAAI*, vol. 1129, 1996, p. 1133.
- [35] T. K. Ho, “The random subspace method for constructing decision forests,” *IEEE T Pattern Anal*, vol. 20, no. 8, pp. 832–844, 1998.
- [36] Z.-H. Zhou, *Ensemble Methods: Foundations and Algorithms*. CRC press, 2012.
- [37] B. Baker, O. Gupta, N. Naik, and R. Raskar, “Designing neural network architectures using reinforcement learning,” in *ICLR*, 2017.
- [38] K. Kandasamy, W. Neiswanger, J. Schneider, B. Poczos, and E. Xing, “Neural architecture search with bayesian optimisation and optimal transport,” in *NeurIPS*, Feb 2018, pp. 2020–2029.
- [39] H. Cai, T. Chen, W. Zhang, Y. Yu, and J. Wang, “Efficient architecture search by network transformation,” in *AAAI*, 2018.
- [40] H. Liu, K. Simonyan, and Y. Yang, “Darts: Differentiable architecture search,” in *ICLR*, 2019. [Online]. Available: <https://openreview.net/forum?id=S1eYHoC5FX>
- [41] A. Zela, A. Klein, S. Falkner, and F. Hutter, “Towards automated deep learning: Efficient joint neural architecture and hyperparameter search,” in *ICML Workshop on AutoML*, 2018.
- [42] K. He, X. Zhang, S. Ren, and J. Sun, “Deep residual learning for image recognition,” in *CVPR*, 2016, pp. 770–778.
- [43] H. Cai, J. Yang, W. Zhang, S. Han, and Y. Yu, “Path-level network transformation for efficient architecture search,” in *ICML*, June 2018.
- [44] E. Real, A. Aggarwal, Y. Huang, and Q. Le, “Regularized evolution for image classifier architecture search,” in *AAAI*, vol. 33, no. 01, 2019, pp. 4780–4789.
- [45] T. Elsken, J. H. Metzen, and F. Hutter, “Efficient multi-objective neural architecture search via lamarckian evolution,” in *ICLR*, 2019. [Online]. Available: <https://openreview.net/forum?id=ByME42AqK7>
- [46] A. Brock, T. Lim, J. Ritchie, and N. Weston, “Smash: One-shot model architecture search through hypernetworks,” in *NIPS Workshop on Meta-Learning*, 2017.
- [47] T. Elsken, J. Metzen, and F. Hutter, “Simple and efficient architecture search for convolutional neural networks,” in *NIPS Workshop on Meta-Learning*, 2017.
- [48] Z. Zhong, J. Yan, W. Wu, J. Shao, and C.-L. Liu, “Practical block-wise neural network architecture generation,” in *CVPR*, 2018, pp. 2423–2432.
- [49] H. Pham, M. Guan, B. Zoph, Q. Le, and J. Dean, “Efficient neural architecture search via parameter sharing,” in *ICML*, 2018.
- [50] Z. Zhong, Z. Yang, B. Deng, J. Yan, W. Wu, J. Shao, and C.-L. Liu, “Blockqnn: Efficient block-wise neural network architecture generation,” *IEEE T Pattern Anal*, 2020.
- [51] J. Chang, X. Zhang, Y. Guo, G. Meng, S. Xiang, and C. Pan, “Differentiable architecture search with ensemble gumbel-softmax,” *arXiv preprint arXiv:1905.01786*, 2019.

- [52] R. Ardywibowo, S. Boluki, X. Gong, Z. Wang, and X. Qian, "Nads: Neural architecture distribution search for uncertainty awareness," in *ICML*. PMLR, 2020, pp. 356–366. [Online]. Available: <https://openreview.net/forum?id=rJeXDANKwr>